Journal of Sports Sciences, May 2006; 24(5): 479 – 493

Taylor & Francis
Taylor & Francis Group

Fixed versus free-floating stretcher mechanism in rowing ergometers: Mechanical aspects

F. COLLOUD[1], P. BAHUAUD[2], N. DORIOT[1], S. CHAMPELY[3], & L. CHÈZE[1]

[1]*Laboratoire de Biomécanique et de Modélisation Humaine, Université Claude Bernard Lyon 1, Villeurbanne,* [2]*Cellule de Biomécanique et de Dynamométrie, Centre des Sports, INSA – Lyon, Villeurbanne, and* [3]*Centre de Recherche et d'Innovation sur le Sport, Université Claude Bernard Lyon 1, Villeurbanne, France*

(Accepted 20 May 2005)

Abstract
The mechanical responses (i.e. external contact forces and external power) of 25 elite rowers to a race-pace rowing protocol were investigated on the traditional fixed stretcher mechanism and the more recently introduced free-floating stretcher mechanism rowing ergometers. Using a Rowperfect rowing ergometer for both conditions, external contact forces at the handle, stretcher and sliding seat, as well as the displacements of the handle and stretcher, were recorded. The external power was calculated as the product of the force and velocity data from both the handle and stretcher. Significant differences ($P < 0.05$) between the two conditions for each mechanical parameter were observed. The fixed condition showed larger maximum values for forces and external power and average power throughout the rowing cycle. Moreover, rowing with the fixed mechanism generated higher inertial forces during the transition between the propulsion and recovery phases, especially at the catch of the cycle. The results suggest that: (i) muscular coordination may differ according to the stretcher mechanism used, which could have an impact on the physiological adaptations of muscles; and (ii) the free-floating mechanism may induce lower catch and maximum values for net joint forces and net joint moments that could decrease the risk of injury.

Keywords: *Biomechanics, rowing, elite, face, power*

Introduction

Competitive rowing requires commitment from athletes over several years and developing the necessary skills and aptitudes (such as physiological, technical and psychological parameters) is a long process. Steinacker, Lormes, Lehmann and Altenburg (1998) reported that as much as 3 hours of on-water training per day is necessary before World Championships. However, winter weather conditions often require both non-specific and semi-specific rowing training. Semi-specific training is usually performed on a rowing ergometer, which provides a sheltered environment and a reasonable alternative to on-water rowing.

Rowing ergometer design has evolved in an attempt to reproduce the movements and load conditions of on-water rowing. Until recently, all rowing ergometers had a fixed stretcher. The two most popular fixed stretcher rowing ergometers have been the Gjessing (A.S. Haby, Norway) and the Concept 2 (Morrisville, VT, USA). The relevance of their physiological responses in comparison with on-water conditions has been widely documented, notably by Secher (1993) and Steinacker (1993). This physiological similarity with on-water rowing has meant that this ergometer design has been very successful. These fixed-stretcher ergometers are currently used for training, performance assessment, and both physiological and biomechanical research programmes. Mechanical conditions are usually investigated by collecting the force generated at the handle (e.g. Hartman, Mader, Wasser, & Klauer, 1993; Hawkins, 2000; Torres-Moreno, Tanaka, & Penney, 2000). In contrast, few studies have recorded the force generated at the stretcher (Macfarlane, Edmond, & Walmsley, 1997) and the force applied on the sliding seat (Pudlo, Barbier, & Angue, 1996). No study has carried out a detailed comparison of these external contact forces with on-water measurement and/or theory. Moreover, the above studies did not take into account the on-water technical skill factor.

Rowing is a cyclic movement that can be separated into two distinct phases, propulsion and recovery.

Correspondence: F. Colloud, Laboratoire Sport et Performance Motrice – EA 597, UFR STAPS, Université Joseph Fourier Grenoble 1, 1741 Rue de la Piscine, BP 53, 38041 Grenoble, France. E-mail: floren.colloud@ujf-grenoble.fr

ISSN 0264-0414 print/ISSN 1466-447X online © 2006 Taylor & Francis
DOI: 10.1080/02640410500189256

The propulsion phase begins at the catch position (i.e. full flexion of the lower limb and lumbar joints and full extension of the upper limb joints) and ends at the finish position (i.e. full extension of the lower limb and lumbar joints and full flexion of the upper limb joints). The propulsion phase involves muscular actions to extend the ankle, knee, hip and lumbar joints and flex the elbow and shoulder joints. The recovery phase is the return of the rower from the finish position to the catch position of the following cycle. As a result, rowing is a complex activity that requires coordinated actions of the trunk, upper and lower limb muscles, which recruit approximately 70% of the body's muscle mass (Steinacker *et al.*, 1998).

With on-water rowing, rower motion relative to a frame embedded in the boat is opposite to boat displacement during the recovery. First, the rower accelerates his centre of mass towards the stern of the boat causing, according to Newton's third law, a reaction force at the stretcher towards the bow of the boat. Then, the rower's centre of mass is decelerated before the catch of the next cycle, resulting in a reaction force towards the stern of the boat. As a result of the rower motion, the velocity of the boat reaches a maximum value during the recovery and is minimal at the catch. A decrease in the fluctuation of the boat velocity results in improved on-water performance (Millward, 1987). The rower's technique may have important negative effects, especially at the time of two inversions in the rowing cycle (i.e. catch and finish) due to the displacement of the limbs' inertial mass. These negative effects have no consequence on a fixed ergometer, since the rower's movement during the recovery does not influence the performance. Although the kinematics of the lower limbs and trunk are similar (Lamb, 1989), this significant mechanical variation could explain the different sensations rowers experience between on-water rowing and on a fixed ergometer, as reported previously by Mahony, Donne and O'Brien (1999).

A rowing ergometer has recently been designed with a free-floating mechanism to improve the simulation of on-water dynamic conditions. The free-floating stretcher has been designed with a view to integrate the rower's motion as a discriminating skill factor. Mahony *et al.* (1999) reported a similar physiological impact when comparing the fixed and the free mechanisms. However, no extensive investigation of the mechanical properties of this new ergometer has been conducted.

The aim of this study was to analyse the external contact forces and external mechanical power using a Rowperfect rowing ergometer (Care, The Netherlands) fitted with either a fixed or a free-floating stretcher mechanism. The innovative free-floating stretcher was compared with the classical fixed stretcher in terms of mechanics during the complete rowing cycle (i.e. propulsion and recovery).

Materials and methods

Participants and test procedure

Twenty-five males (age 23.7 ± 3.1 years, height 1.84 ± 0.06 m, body mass 80.6 ± 8.5 kg; mean $\pm$ *s*) volunteered to participate in this study, some ($n = 18$) with international experience and others ($n = 7$) with experience of the national championships. The frequency of training sessions ranged from 9 to 13 per week. All participants had performed an all-out 2000 m rowing test (6:13 $\pm$ 0:11 min:s) on a fixed rowing ergometer (Concept 2, Model C) as part of national training programmes 4 months before this experiment.

The participants completed the following rowing ergometer test schedule. After a warm-up, they performed two 15-cycle race-pace tests (35 cycles $\cdot$ min^{-1}; Steinacker, 1993) on a Rowperfect rowing ergometer. In randomized order, each rower performed one test on the Rowperfect fitted with a free-floating stretcher mechanism and one fitted with a fixed stretcher mechanism. Using the same kind of rowing ergometer for both conditions (fixed vs. free-floating stretcher mechanisms) decreased the number of variables in the comparison (i.e. type of resistance system that rowers must overcome, rower's set-up). Accordingly, the comparison could focus on the mechanical effects caused by the two stretcher mechanisms during the rowing cycle.

The participants received real-time graphical and numerical information feedback of their performances (cycle rate, power per cycle, force – time curve). The participants were asked to perform using their usual rowing technique, especially in terms of cycle length and cycle rhythm, to simulate as closely as possible race-pace conditions. All computations were done using Matlab software (The Math Works, Natick, MA, USA).

Data acquisition

Kinematic data processing. The position and the orientation of the handle and stretcher were defined respectively by three reflective non-aligned markers (diameter 20 mm). The flywheel axis position was reconstructed using the positions of the three markers placed on the stretcher. Their three-dimensional trajectories were captured using a video-based motion analysis system (Motion Analysis Corporation, Santa Rosa, CA, USA), equipped with six "near red" cameras. This motion analysis system computes the three-dimensional trajectories of the reflective markers with a dynamic accuracy of 2 mm (Richards, 1999).

The position data were filtered using a Butterworth digital filter (cut-off frequency = 5 Hz) to eliminate the high-frequency noise caused by the measurement system. The cut-off frequency was consistent with a maximum of 0.75 Hz for the rowing movement (Martindale & Robertson, 1984).

Force data processing. The Rowperfect rowing ergometer was specifically instrumented to measure the external contact forces between the ergometer and the rower (see Figure 1). To record the force generated by the handle on the two hands ($\boldsymbol{F_{handle}}$), a strain gauge force transducer (Interface SM 100 N, measurement range 1000 N, tolerance of overload 500 N) was connected in series with the chain and the handle, using a ball and socket joint (i.e. three degrees of freedom in rotation). The force transducer had a stated linearity of 0.03% and hysteresis of 0.02%. The handle force was decomposed into antero-posterior (F^{ap}_{handle}) and vertical (F^{vert}_{handle}) components using the line of pull. The line of pull was computed as the line from the handle position to the flywheel axis position, θ being the angle between this line and the antero-posterior axis $\boldsymbol{X_0}$.

The stretcher was fitted with four (specifically developed) bi-directional (antero-posterior and vertical axes) strain-gauge transducers (measurement range 1500 N, tolerance of overload 750 N, linearity 0.15%, hysteresis 0.02%) to record the stretcher force on the rower ($\boldsymbol{F_{stretcher}}$). The antero-posterior ($F^{ap}_{stretcher}$) and vertical ($F^{vert}_{stretcher}$) stretcher forces were calculated using the data provided by the stretcher transducers. The magnitude of the stretcher force ($||\boldsymbol{F_{stretcher}}||$), together with the angle between the stretcher force and the antero-posterior axis (α), were then computed.

To measure the vertical force applied by the sliding seat on the rower's ischia (F^{vert}_{seat}), a frame fitted with three small load cells (Sensotec S3E, measurement range 1000 N, tolerance of overload 500 N, linearity 0.25%, hysteresis 0.2%) was placed under the sliding seat.

The force signals were sampled by an acquisition device (SOMAT 2100 Turbo, Johne + Reihofer) and digitally stored using the Test Control SOMAT software on a laptop computer.

Before data collection, each strain gauge force transducer was calibrated using known weights: 452.2 N, 750 N and 1000 N for stretcher, seat and handle force transducers, respectively. The zero reference of the force transducers was collected before each rower's test procedure. The linearity and the hysteresis of each strain gauge force transducer were recorded in test configuration – that is, the acquisition device measured the characteristics of the force transducer fitted to the ergometer with the specially developed frame.

To record a stabilized rowing cycle, data collection began five cycles after the start of the test (Hartman *et al.*, 1993; Millward, 1987). Motion and force data were captured at a sampling frequency of 60 Hz for 10 s. This ensured the collection of at least three complete cycles for analysis. The acquisition of kinematic and force data was synchronized by a unique and common start impulse.

Modelling

Free body analysis. Five forces act on the rower's body: rower's weight ($\boldsymbol{W_{rower}} = m_{rower} \cdot \boldsymbol{g}$, where m_{rower} is the rower's mass and $\boldsymbol{g}$ is the gravitational acceleration), air resistive force ($\boldsymbol{F_{air}}$) and three external contact forces, at the handle ($\boldsymbol{F_{handle}}$), the stretcher ($\boldsymbol{F_{stretcher}}$) and the sliding seat ($\boldsymbol{F_{seat}}$). The rower generates the stretcher force directly and acts

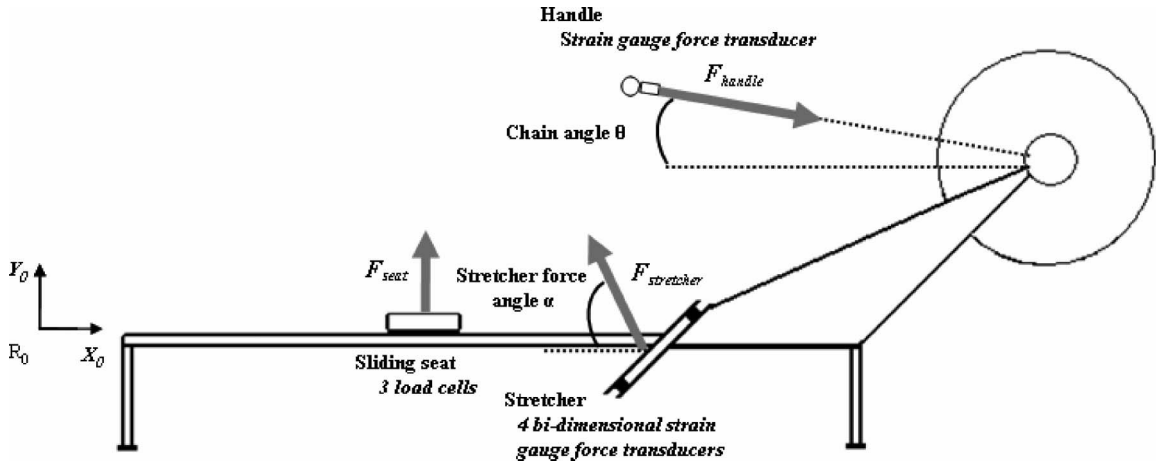

Figure 1. Schematic representation of the modified Rowperfect rowing ergometer instrumented to measure the external contact forces between the ergometer and the rower. $\boldsymbol{F_{handle}}$, $\boldsymbol{F_{stretcher}}$ and $\boldsymbol{F_{seat}}$ are the forces exerted by the handle, stretcher and sliding seat on the rower. These forces are projected in the laboratory frame $R_0 = (\boldsymbol{OX_0Y_0})$. θ is the angle between $\boldsymbol{F_{handle}}$ and $\boldsymbol{X_0}$. α is the angle between $\boldsymbol{F_{stretcher}}$ and $\boldsymbol{X_0}$.

as a mechanical link between the stretcher force and the handle force.

The forces and moments acting on the rower were considered only in the sagittal plane, $R_0 = (O\boldsymbol{X_0}\boldsymbol{Y_0})$. It was assumed that the friction forces generated at the sliding seat and stretcher during the rowing cycle as well as the air resistive force were minimal and thus neglected. Thus, there are only two antero-posterior forces acting on the rower during the propulsion phase (equation 1), whereas all the forces act according to the vertical axis ($O\boldsymbol{Y}_0$) (equation 2). The vertical forces cannot be neglected since Nolte (1991) has shown vertical movement of the rower's centre of mass (COM). From a quasi-static approximation, the sum of the moments acting on the rower expressed at the rower's centre of mass is shown in equation (3).

The sagittal plane equations of motion (a quasi-static approximation in the case of the rotational equation) governing the movement of the rower during the complete rowing cycle are as follows:

$$F^{ap}_{handle} + F^{ap}_{stretcher} = m_{rower} \cdot a^{ap}_{COM} \quad (1)$$

$$F^{vert}_{handle} + F^{vert}_{stretcher} + F^{vert}_{seat} + W_{rower} = m_{rower} \cdot a^{vert}_{COM} \quad (2)$$

$$-F^{ap}_{handle} \cdot d^{ap}_{handle} + F^{vert}_{handle} \cdot d^{vert}_{handle} - F^{ap}_{stretcher} \cdot d^{ap}_{stretcher} + F^{vert}_{stretcher} \cdot d^{vert}_{stretcher} + F^{vert}_{seat} \cdot d^{vert}_{seat} = 0 \quad (3)$$

where a^{ap}_{COM} and a^{vert}_{COM} are the antero-posterior and vertical accelerations of the rower's centre of mass, d^{ap} is the moment arm of the antero-posterior forces and d^{vert} is the moment arm of the vertical forces. d^{ap} and d^{vert} are defined by equations (4) and (5):

$$d^{ap} = yA - yCOM \quad (4)$$

$$d^{vert} = xA - xCOM \quad (5)$$

where xA and yA are the antero-posterior and vertical coordinates in the reference frame R_0 of the point of application of handle, stretcher and seat forces, respectively, and $xCOM$ and $yCOM$ are the antero-posterior and vertical coordinates in the reference frame R_0 of the rower's centre of mass. Figure 2 shows the forces and moments that acted on the rower in the sagittal plane $R_0 = (O\boldsymbol{X_0}\boldsymbol{Y_0})$ at mid-propulsion of the rowing cycle.

External power. From the external forces and kinematics data, the external power (P_{ext}) generated by the rower was computed. P_{ext} was defined by equation (6) as:

$$P_{ext} = -F^{ap}_{handle} \cdot V^{ap}_{handle} - F^{vert}_{handle} \cdot V^{vert}_{handle} - F^{ap}_{stretcher} \cdot V^{ap}_{stretcher} \quad (6)$$

where V^{ap}_{handle} and $V^{ap}_{stretcher}$ are the horizontal velocities of the handle and stretcher respectively and V^{vert}_{handle} is the vertical velocity of the handle expressed with respect to the reference frame R_0. As explained above, the friction forces generated at the sliding seat and stretcher were neglected. The powers associated with each cycle were divided by the time per cycle to provide the average power.

Fixed versus free-floating stretcher mechanisms

The Rowperfect rowing ergometer is an air-braked flywheel ergometer. The flywheel is drawn by a self-recoiling chain connected to a handle. The sliding seat has two degrees of freedom: one in translation and one in rotation with respect to the central sliding bar. Consequently, the rower has to balance his load on the sliding seat during the rowing cycle.

Free-floating stretcher mechanism. The Rowperfect differs from a conventional rowing ergometer by having a free stretcher mechanism that slides along the central bar. The free mechanism includes the stretcher and the flywheel bound to the stretcher by a metal link. The mass of this system (17.5 kg) is close to that of a skiff and its two sculls.

In the reference frame R_0 (see Figure 3), the stretcher is pushed forward by the rower during propulsion and pulled back during recovery. Although the seat can slide freely, the translation remains minimal when this ergometer is rowed by a skilled rower. In other words, the displacement of the rower's centre of mass is minimal during the cycle. As a result, the two antero-posterior forces must be in equilibrium (equation 1). Failure to equate these forces causes a large displacement along the slide bar of both the sliding seat and the free mechanism. In the latter case, the free mechanism, and more rarely the sliding seat, reaches the extremities of the slide bar.

Fixed stretcher mechanism. The Rowperfect was transformed into a conventional fixed stretcher ergometer by placing a clamp underneath the free mechanism and attaching it to the front stand. During the cycle, the motion of the rower is very different from that in the free condition. The rower pushes against a fixed point in the laboratory frame R_0 and moves backward during propulsion and pull to move forward during recovery (see Figure 3). This means that the rower's centre of mass is translated along the central bar, relative to the stretcher, during the rowing cycle.

Analysis of results

Three successive cycles were selected and analysed from the two rowing conditions. Rowing cycles

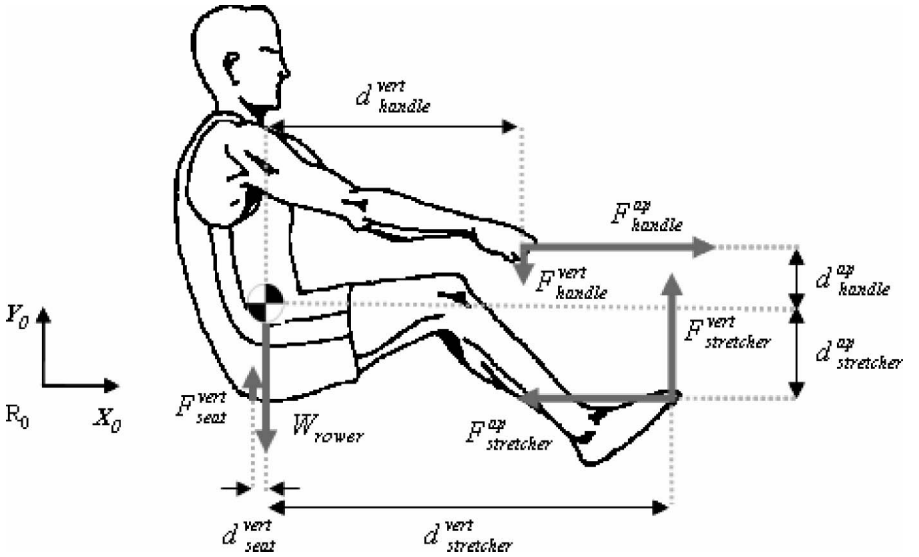

Figure 2. Rower's weight ($\boldsymbol{W_{rower}} = \boldsymbol{m}_{\text{rower}} \cdot \boldsymbol{g}$) together with handle ($F^{ap}_{handle}$, F^{vert}_{handle}), stretcher ($F^{ap}_{stretcher}$, $F^{vert}_{stretcher}$) and sliding seat (F^{vert}_{seat}) forces acting on the rower at mid-propulsion and their moment arms about the rower's centre of mass (d^{ap}_{handle}, $d^{vert}_{stretcher}$, $d^{ap}_{stretcher}$, $d^{vert}_{stretcher}$, d^{vert}_{seat}) in the sagittal plane $R_0 = (O\boldsymbol{X_0Y_0})$.

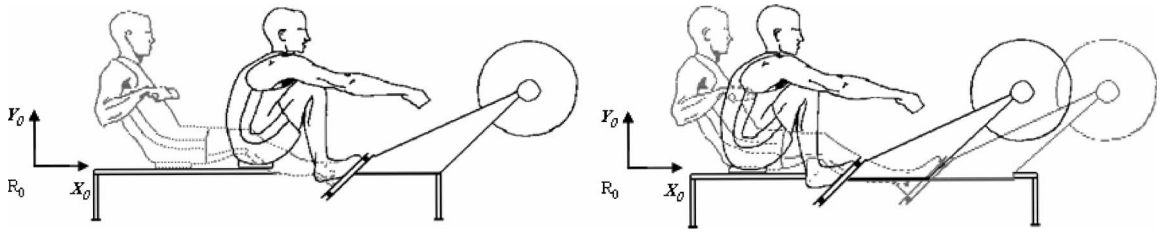

Figure 3. Schematic representation of the positions at the catch (continuous line) and the finish (dotted lines) on a fixed stretcher mechanism (left) and a free-floating stretcher mechanism (right). In the free-floating condition, during the propulsion phase, the stretcher moves forward relative to the laboratory frame $R_0 = (\boldsymbol{OX_0}Y_0)$, whereas the sliding seat translation remains minimal. In the fixed condition, inverted motion is obtained: the stretcher is fixed to the laboratory frame and the seat slides backwards.

(propulsion and recovery) were accurately identified by the antero-posterior displacement in the reference frame R_0 of the handle relative to the stretcher. The catch and the finish of the cycles corresponded to the successive times at which the velocity of the handle relative to the stretcher projected in R_0 was zero. For each cycle, the desired variables [i.e. handle position (antero-posterior position in the reference frame R_0 of the handle relative to the stretcher); handle velocity relative to the stretcher; handle, stretcher and sliding seat forces; magnitude and angle with the antero-posterior axis of the stretcher force; handle and stretcher external powers; rower's centre of mass and stretcher antero-posterior accelerations] were time-normalized on the interval [0, 1] and time-averaged for the 25 rowers. All these variables were expressed in the reference frame $R_0 = (O\boldsymbol{X_0Y_0})$. Then, the profiles of the variable cycle as a function of the handle position were constructed; 95% confidence intervals were included to indicate variability across participants (see Figures 4–9). From Figures 4–9, one can see that the handle position (i.e. antero-posterior position of the handle relative to the stretcher in the reference frame R_0 – horizontal axes) was slightly positive at the catch as the handle was situated ahead of the stretcher in R_0 (see Figure 3). Conversely, at the finish, the handle was situated behind the stretcher in R_0, resulting in a negative value for the handle position. On the horizontal axis, a zero value indicates that the handle was placed directly above the stretcher.

Discrete mean values represented the mean of the analysed variables achieved by the 25 rowers during the rowing cycle. These discrete variables included maximum and minimum values, the handle positions at which they occurred, the catch and finish values, the cycle variables (cycle rate and cycle length), as well as the average power throughout the complete rowing cycle and the rower's mean centre of mass antero-posterior acceleration.

Statistical analysis

For each mean discrete variable, the significance of the difference was tested using a paired Student's *t*-test. A significant difference between the two experimental conditions was recorded when the *P*-value was below 0.05.

Results

Cycle characteristics

To validate the test procedure, the cycle rate (*CR*) was calculated from the number of cycles performed (*CN*) and the total time of the cycles (*T*):

$$CR = CN \cdot T^{-1} \tag{7}$$

The imposed cycle rate (35 cycles $\cdot$ min^{-1}) was correctly maintained by all participants for the two ergometer conditions: 34.4 ± 1.4 and 35.5 ± 1.4 cycles $\cdot$ min^{-1} for the fixed and the floating mechanisms respectively. The propulsion phase represented $48.0 \pm 1.7\%$ of the rowing cycle for both experimental conditions ($P > 0.05$). The cycle length, defined as the absolute antero-posterior displacement of the handle relative to the stretcher from catch to finish, was higher during the fixed condition (1.44 ± 0.07 m) than during the free-floating condition (1.41 ± 0.08 m) ($P < 0.05$).

Forces at the handle

Table I presents the average maximum and minimum forces collected on the handle and on the stretcher and the handle positions at which they occurred, during the rowing cycle for the two rowing ergometer tests.

Figure 4 displays the average curves of the antero-posterior (F^{ap}_{handle}) and vertical (F^{vert}_{handle}) forces generated at the handle for the two rowing tests. The handle force cycle profiles were similar for all participants, as indicated by the 95% confidence intervals. The F^{ap}_{handle} curves showed a bell shape with a rapid rise in the magnitude of force until reaching a peak, followed by a decrease (see Figure 4 top) and minimal values during the recovery phase. F^{vert}_{handle} was negative in the propulsion phase. As a result, the F^{vert}_{handle} curves showed a reverse bell shape (see Figure 4 bottom). Moreover, F^{vert}_{handle} represented, on average, $14 \pm 7\%$ of F^{ap}_{handle} for both conditions. F^{ap}_{handle} was significantly higher with the fixed stretcher mechanism for a handle displacement of 0.40 m (handle positions -0.54 to -0.94 m) during the propulsion phase. F^{ap}_{handle} lay outside the 95% confidence intervals, indicating F^{ap}_{handle} with the fixed mechanism is significantly greater for 30% of the cycle length during the propulsion phase.

Table I. Comparison of the mean maximum and minimum forces collected on the handle, the stretcher and the sliding seat and the handle positions at which they occurred (i.e. antero-posterior position of the handle relative to the stretcher in the reference frame R_0) for the fixed and the free-floating mechanisms.

	Maximum force (N) (mean $\pm$ *s*)		Handle position (m) (mean $\pm$ *s*)		Minimum force (N) (mean $\pm$ *s*)		Handle position (m) (mean $\pm$ *s*)	
	Fixed	Floating	Fixed	Floating	Fixed	Floating	Fixed	Floating
F^{ap}_{handle}	1134 ± 108	1054 ± 75**	-0.63 ± 0.08	-0.62 ± 0.09	—	—	—	—
F^{vert}_{handle}	—	—	—	—	-184 ± 36	-171 ± 28**	-0.49 ± 0.07	-0.49 ± 0.07
$F^{ap}_{stretcher}$	235 ± 68	31 ± 61**	-0.97 ± 0.17	-0.67 ± 0.47**	-908 ± 207	-951 ± 247	-0.62 ± 0.14	-0.67 ± 0.16
$F^{vert}_{stretcher}$	791 ± 184	690 ± 162**	-0.24 ± 0.20	-0.39 ± 0.15**	-190 ± 95	-71 ± 58**	-1.09 ± 0.08	-1.10 ± 0.11
F^{vert}_{seat}	1034 ± 123	924 ± 157**	-1.16 ± 0.09	-1.13 ± 0.11	80 ± 42	103 ± 63	-0.09 ± 0.22	-0.44 ± 0.11**

Note: Significant difference between the fixed and free-floating stretcher mechanisms: *$P < 0.05$, **$P < 0.01$.
Abbreviations: F^{ap}_{handle} and F^{vert}_{handle}: antero-posterior and vertical forces generated by the handle on the two hands; $F^{ap}_{stretcher}$ and $F^{vert}_{stretcher}$: antero-posterior and vertical forces generated by the stretcher on the two feet; F^{vert}_{seat}: vertical force generated by the sliding seat on the rower.

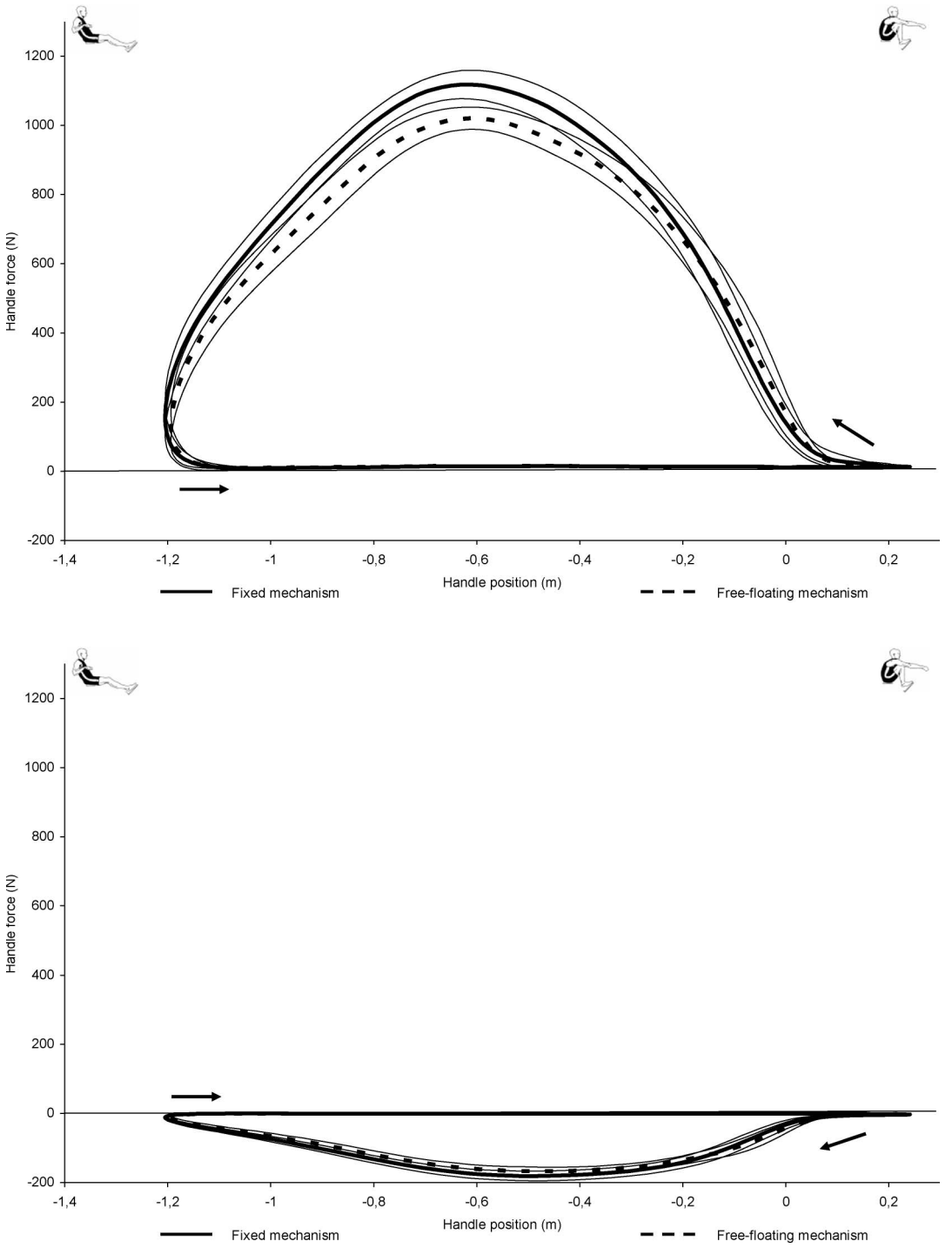

Figure 4. Mean curves of the forces generated by the handle on the 25 rowers as a function of handle position (i.e. antero-posterior position of the handle relative to the stretcher in the reference frame R_0). The two ergometer conditions are shown as bold lines with 95% confidence intervals above and below as thin lines; continuous lines represent the fixed condition and dotted lines the free-floating condition. Figures of the rower indicate the catch and finish positions; the arrows indicate the way of reading the curves from these two positions. (Top) Antero-posterior force (F^{ap}_{handle}). (Bottom) Vertical force (F^{vert}_{handle}).

The F^{ap}_{handle} maximal value occurred at the same stage of the cycle (handle position -0.63 m, $P > 0.05$) irrespective of the mechanism used, although the F^{ap}_{handle} maximal value was 7.1% lower ($P < 0.01$) when the participants used the floating mechanism. A similar difference was observed for the F^{vert}_{handle} minimum values between the two conditions (7.1%, $P < 0.01$). The F^{vert}_{handle} minimum values occurred 0.14 m earlier ($P > 0.05$) in the cycle than the F^{ap}_{handle} maximum values.

An unnecessary movement was observed at the catch where no handle forces were collected even though a displacement of the handle was recorded. The floating curves were shifted to the right so that F^{ap}_{handle} and F^{vert}_{handle} started to increase earlier in the cycle (lag in application of handle forces: 0.11 m, 7.7% of the cycle length) compared with the forces recorded in the fixed condition (lag in application of handle forces: 0.18 m, 12.4% of the cycle length). Consequently, F^{ap}_{handle} was applied for longer during the propulsion phase when the rowers were in the free-floating condition. The handle forces observed at the finish were found to be equal to the static traction forces provided by the elasticity of the self-recoiling system measured separately.

Forces at the stretcher

Figure 5 shows the antero-posterior force ($F^{ap}_{stretcher}$) and vertical force ($F^{vert}_{stretcher}$) exerted by the rowers on the stretcher. During the rowing cycle, $F^{ap}_{stretcher}$ and $F^{vert}_{stretcher}$ were opposite: $F^{ap}_{stretcher}$ was negative and $F^{vert}_{stretcher}$ was positive for the propulsion phase, whereas $F^{ap}_{stretcher}$ was positive and $F^{vert}_{stretcher}$ was negative for the recovery phase. Nevertheless, the global shapes of the stretcher force curves depended on the mechanism being used. The two stretcher mechanism conditions showed significant differences for $F^{ap}_{stretcher}$ during approximately 30% of the cycle length in the propulsion phase (handle positions: catch position to -0.00 m and -0.94 m to finish position) and the complete recovery phase. $F^{vert}_{stretcher}$was also significantly different between the two conditions during approximately 30% of cycle length in the propulsion phase (handle positions: catch position to -0.19 m) and again 40% of cycle length in the recovery phase (handle positions: finish position to -0.80 m and -0.01 m to catch position).

At the catch, $F^{ap}_{stretcher}$ and $F^{vert}_{stretcher}$ showed significant differences, with the fixed mechanism having greater $F^{ap}_{stretcher}$ (83.8%, $P < 0.01$) and lower $F^{vert}_{stretcher}$ (51.8%, $P < 0.01$) values. Moreover, each experimental condition had a line of action of the stretcher force mostly oriented vertically as $F^{ap}_{stretcher}$ showed lower absolute values than $F^{vert}_{stretcher}$. The floating condition induced a larger angle (α) between the stretcher force and the antero-posterior axis ($81 \pm 15^{\circ}$) than the fixed condition ($64 \pm 14^{\circ}$) ($P < 0.01$).

During propulsion, $F^{vert}_{stretcher}$ reached its maximum value before $F^{ap}_{stretcher}$ reached its minimum value ($P < 0.01$). The $F^{ap}_{stretcher}$ minimum value occurred at the same stage of propulsion as the F^{ap}_{handle} maximum value ($P > 0.05$), whereas the $F^{vert}_{stretcher}$ maximum value occurred closest to the catch ($P < 0.01$). Compared with the floating condition, larger $F^{vert}_{stretcher}$ maximum values (12.8%, $P < 0.01$) and similar $F^{ap}_{stretcher}$ minimum values (4.5%, $P > 0.05$) were observed when the fixed mechanism was rowed. In addition, the rowers produced similar stretcher maximum force (2.1%, $P > 0.05$) during the two tests.

In contrast to the catch, both conditions showed larger absolute $F^{ap}_{stretcher}$ maximal values compared with maximum $F^{vert}_{stretcher}$ ($P < 0.01$). As a consequence, the stretcher force acted in a more antero-posterior direction during propulsion. The floating stretcher led to a decrease of α until 24° (handle position: -1.05 m), whereas α decreased until 31° (handle position: -0.90 m) for the fixed mechanism.

At the finish of the rowing cycle, $F^{ap}_{stretcher}$ and $F^{vert}_{stretcher}$ recorded negative values. Negative values were also recorded for $F^{vert}_{stretcher}$ during the recovery phase. $F^{vert}_{stretcher}$ was negative for longer when the fixed mechanism was used (handle displacement: fixed 0.87 m, free-floating 0.45 m). $F^{ap}_{stretcher}$ was positive during most of the recovery phase for the fixed mechanism, whereas it was minimal for the floating mechanism. During the recovery phase, α evolved in a different way according to the mechanism rowed. For the floating condition α was close to 80°, whereas for the fixed condition it was larger (close to 135° for a handle position between -1.13 and -0.30 m) and then decreased to the next catch.

Force at the sliding seat

Figure 6 shows a variation of more than 800 N in the loading force applied by the rower on the sliding seat (F^{vert}_{seat}) throughout the rowing cycle. The mean value of F^{vert}_{seat} in the static position was 699 ± 72 N for the 25 participants. The lowest F^{vert}_{seat} values (less than 110 N) were collected during propulsion, whereas the highest values occurred at the finish, followed by a slump until the next catch.

The curves for the 95% confidence intervals indicate that F^{vert}_{seat} on the fixed mechanism was significantly lower during the last part of the recovery phase (handle positions: 0.17 m to catch position) and beginning of the propulsion phase (handle positions: catch position to -0.25 m). For the free-floating condition, the catch and the minimum values were higher (51.4% and 11.4% respectively, $P < 0.01$) and the minimum value occurred 0.35 ± 0.22 m ($P < 0.01$) later in the propulsion phase. Furthermore, the finish value was 11.4% lower ($P < 0.01$).

Dynamic analysis of the rowing cycle

From Figures 4 and 5, it can be seen that the antero-posterior forces generated at the handle and stretcher were not equal and opposite. These variations reflect the effects of the inertia mass of the rower's segments and acceleration of the rower's centre of mass

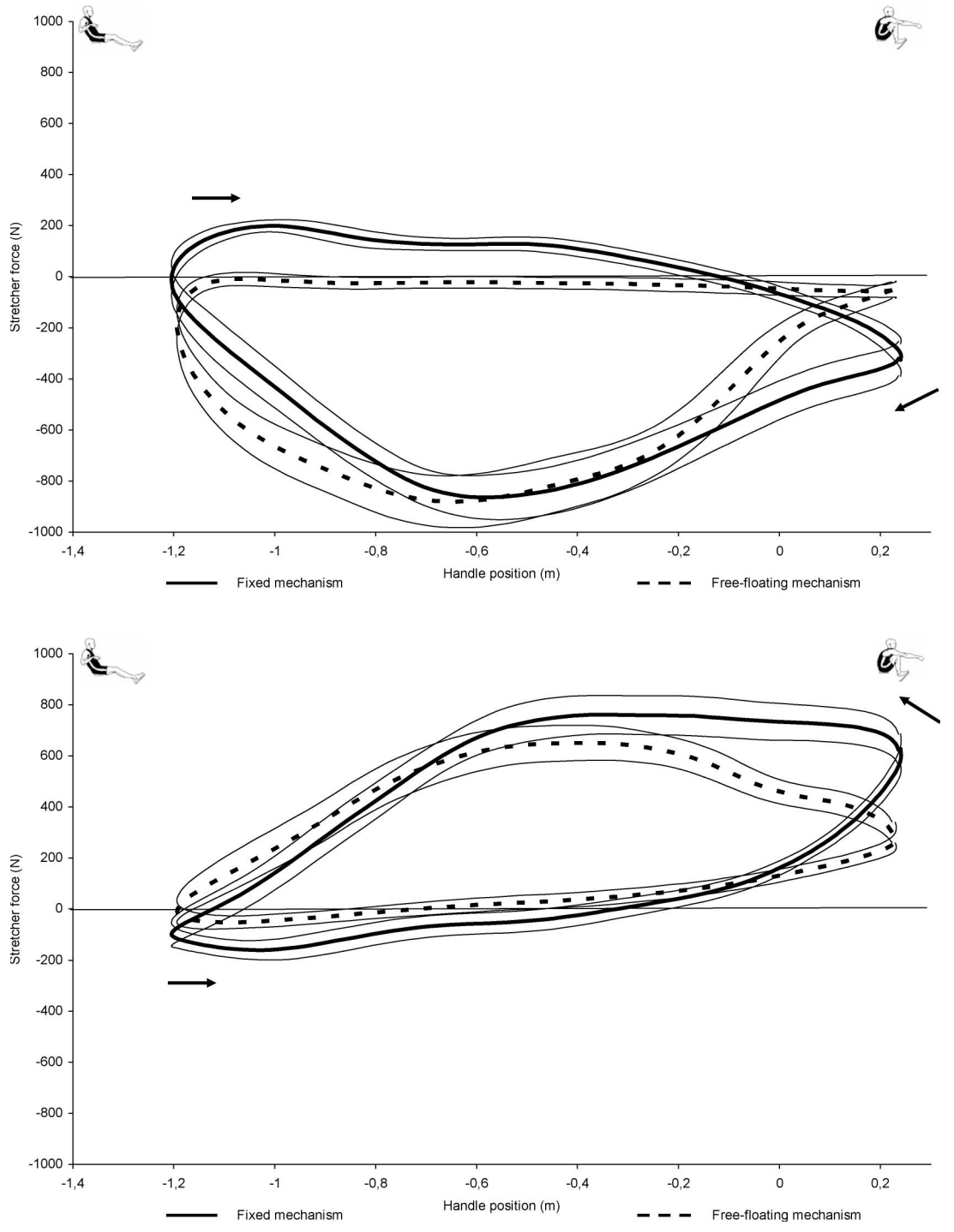

Figure 5. Mean curves of the forces generated by the stretcher on the 25 rowers as a function of handle position. Figures of the rower indicate the catch and finish positions; the arrows indicate the way of reading the curves from these two positions. (Top) Antero-posterior force ($F^{ap}_{stretcher}$). (Bottom) Vertical force ($F^{vert}_{stretcher}$).

throughout the cycle. To analyse these variations, the antero-posterior acceleration of the rower's centre of mass (a^{ap}_{COM}) was isolated from the left term of equation (1). Thus, $a^{ap}_{COM}$is defined as follows:

$$a^{ap}_{COM} = (F^{ap}_{handle} + F^{ap}_{stretcher})/m_{rower} \qquad (8)$$

Figure 7 displays the average curves of a^{ap}_{COM} for the two rowing tests. It must be emphasized that the average curves of a^{ap}_{COM} recorded on both ergometers show large inter-individual variability throughout the propulsion phase. Although all the participants were high-level rowers, they produced

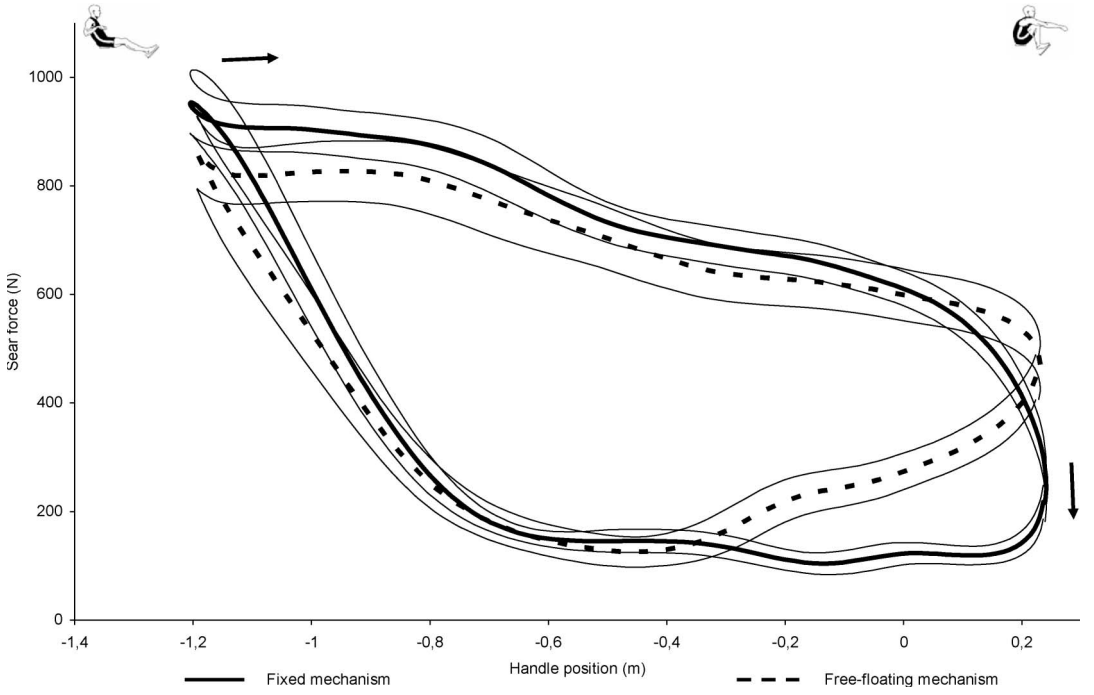

Figure 6. Mean curves of the vertical force applied by the sliding seat on the 25 rowers (F_{seat}^{vert}) as a function of handle position. Figures of the rower indicate the catch and finish positions; the arrows indicate the way of reading the curves from these two positions.

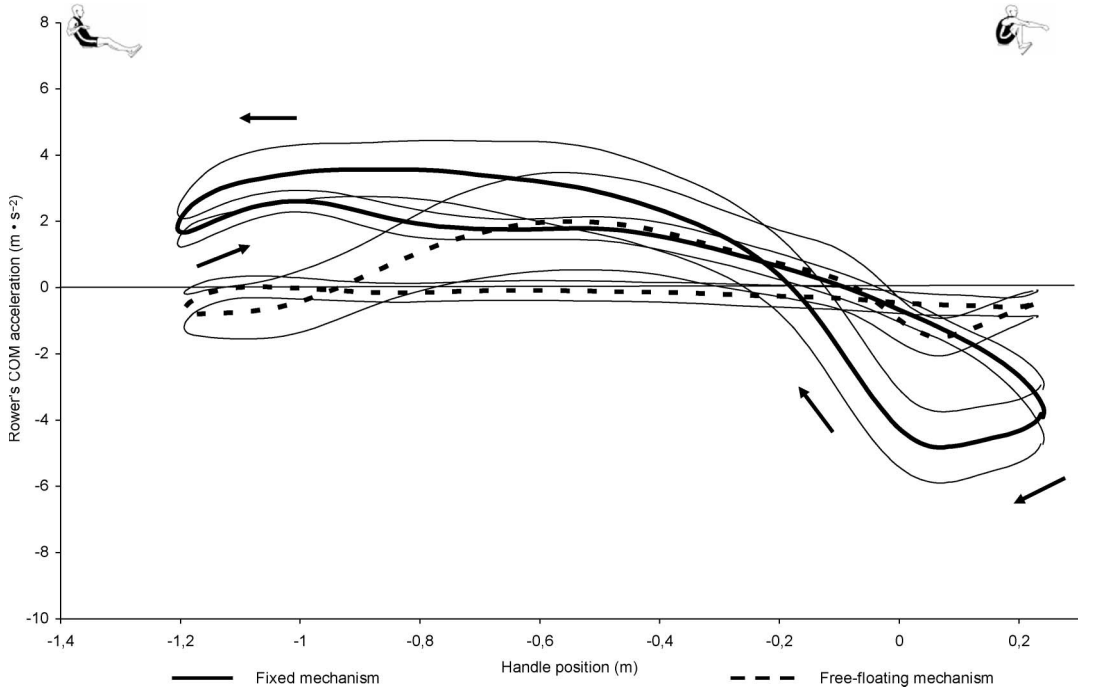

Figure 7. Mean curves of the antero-posterior acceleration of the rower's centre of mass (a_{COM}^{ap}) as a function of handle position. Figures of the rower indicate the catch and finish positions; the arrows indicate the way of reading the curves from these two positions.

widely different synchronization between the antero-posterior forces. In other words, each rower showed different skills and adaptations during the propulsion phase. a_{COM}^{ap} lay outside the 95% confidence intervals during about 50% of the propulsion phase (handle positions: catch position to -0.13 m and -0.80 m to finish position) and the whole of recovery, indicating a_{COM}^{ap} is significantly different between the two stretcher mechanisms for these handle displacements. The average rower's

centre of mass antero-posterior acceleration computed for the complete rowing cycle was close to zero for both conditions (0.4141 ± 0.8922 and $-0.0125 \pm 1.025\,m \cdot s^{-2}$ for the fixed and the floating conditions, respectively).

When the participants rowed with the fixed mechanism, a^{ap}_{COM} was negative for the first 0.40 m of the cycle (minimum value: $-5.4 \pm 2.2\,m \cdot s^{-2}$; handle position: 0.01 ± 0.22 m) (see Figure 7). Similarly, the last 0.31 m of the recovery phase was also characterized by negative values, which means the rower pushed on the stretcher whereas the magnitude of the handle force was minimal. As a consequence, the antero-posterior force generated at the stretcher acted to decelerate the rower's centre of mass at the end of the recovery/beginning of the propulsion phase. For the rest of the rowing cycle, a^{ap}_{COM} was positive (maximum value: $5.5 \pm 1.7\,m \cdot s^{-2}$; handle position: -0.86 ± 0.25 m) and thus the rower's centre of mass was accelerated. At the end of the propulsion phase, some of the rower's centre of mass acceleration was supplied by the handle force. Next, the rower pulled on the stretcher to initiate the recovery phase causing large positive values of a^{ap}_{COM} as the force applied on the handle was minimal.

For the floating mechanism, a^{ap}_{COM} was characterized by smaller values throughout the rowing cycle [minimum value: $-2.5 \pm 1.2\,m \cdot s^{-2}$ ($P < 0.01$), handle position: -0.53 ± 0.58 m ($P < 0.01$); maximum value: 2.9 ± 2.6 ($P < 0.01$), handle position: -0.58 ± 0.35 m ($P < 0.01$)] and less inertia force was generated by the rower, namely at the two inversions of the cycle [catch: $0.1 \pm 0.1\,m \cdot s^{-2}$ vs. $-3.8 \pm 2.1\,m \cdot s^{-2}$ ($P < 0.01$); finish: $-0.8 \pm 1.1\,m \cdot s^{-2}$ vs. $1.9 \pm 1.4\,m \cdot s^{-2}$ ($P < 0.01$) for the free-floating vs. fixed mechanism). The rower's centre of mass was decelerated during the first 0.27 m and the later stages of the propulsion phase (0.25 m of the cycle length, a^{ap}_{COM} minimum value: $-0.80\,m \cdot s^{-2}$). a^{ap}_{COM} was positive during the rest of the propulsion phase and minimal for the major part of the recovery phase.

The variations of the vertical forces reflect mainly the changing distribution of the rower's weight (see equation 2). From Figures 4, 5 and 6 it can be seen that the way in which the vertical handle and seat forces change was opposite to the stretcher vertical force. This means that the main support point for the rower throughout the propulsion phase was the stretcher. The rower has to balance the large clockwise moment generated by the handle forces and the stretcher antero-posterior force (see Figure 2). The vertical stretcher and seat forces are the two forces that can create an anti-clockwise moment. This anti-clockwise moment is only due to the vertical stretcher force during the first part of the propulsion phase (following equation 3), the seat force creating an anti-clockwise moment for the last part of the propulsion phase, near the finish.

The sliding seat load reached its maximum at the finish, when the lower limbs and trunk were fully extended. The inertial force created by the rotational motion of the trunk at the end of the propulsion phase was balanced by vertical stretcher force to initiate the recovery. As the rower has to overcome less inertial force for the first part of the propulsion phase, the free-floating mechanism induces lower vertical force at the stretcher and lower variation of the load at the sliding seat.

External power

The shape of the external power curves (P_{ext}) characterizes each of the mechanisms rowed (see Figure 8). A low variability across participants was observed for the two conditions as indicated by the 95% confidence intervals. The external power on the fixed stretcher was significantly lower for the first 20% or so of the cycle length in the propulsion phase (handle positions: catch position to -0.06 m). Then, the rowers produced an external power significantly greater for about 30% of the cycle length (handle positions: -0.46 to -0.94 m) and for the last 20% of the cycle length in the recovery phase (handle positions: -0.06 to catch position). Table II presents the minimum and maximum values and the handle positions at which they occurred during the rowing cycle for external power, power delivered at the handle in the antero-posterior and vertical directions (P^{ap}_{handle} and P^{vert}_{handle} respectively) and power delivered at the stretcher in the antero-posterior direction ($P^{ap}_{stretcher}$). These variables were computed for the two ergometer conditions. In Table II and Figure 8, the generated powers took positive values and the absorbed powers negative values.

The shape of the curve computed from the fixed condition was similar to the shape of F^{ap}_{handle}, (i.e. a bell shape). In this condition, P_{ext} was mainly produced by the pulling force and the antero-posterior velocity of the handle. P^{ap}_{handle} maximum power was similar to the P_{ext} maximum value ($P > 0.05$), although P^{ap}_{handle} maximum power occurred earlier in the rowing cycle ($P < 0.01$). The stretcher generated a minimal power that was caused by some slip (inferior to 5 mm) of the ergometer on the floor during the rowing cycle. The recovery was characterized by a small power absorbed by the rower.

As observed previously for $F^{ap}_{stretcher}$, the P_{ext} curve corresponding to the free-floating condition began to increase earlier in the rowing cycle. During the first part of the propulsion phase, $P^{ap}_{stretcher}$ was predominant and then the majority of P_{ext} was

Table II. Comparison of the mean maximum and minimum forces and the handle positions at which they occurred (i.e. antero-posterior position of the handle relative to the stretcher in the reference frame R_0) computed for external power, handle power and stretcher power for the fixed and the free-floating mechanisms.

	Maximum power (W) (mean ± s)		Handle position (m) (mean ± s)		Minimum power (W) (mean ± s)		Handle position (m) (mean ± s)	
	Fixed	Floating	Fixed	Floating	Fixed	Floating	Fixed	Floating
P^{ap}_{handle}	2491 ± 299	1633 ± 187**	−0.66 ± 0.09	−0.77 ± 0.06**	−50 ± 28	−36 ± 37	−0.74 ± 0.31	−0.82 ± 0.19
P^{vert}_{handle}	25 ± 16	29 ± 19*	−0.29 ± 0.14	−0.30 ± 0.15	−26 ± 12	−22 ± 11*	−0.85 ± 0.10	−0.84 ± 0.20
$P^{ap}_{stretcher}$	13 ± 12	838 ± 275**	−0.31 ± 0.56	−0.42 ± 0.11	−17 ± 6	−68 ± 50**	−0.39 ± 0.25	−0.18 ± 0.46*
P_{ext}	2482 ± 306	2174 ± 283**	−0.65 ± 0.08	−0.66 ± 0.08	−51 ± 28	−84 ± 55**	−0.79 ± 0.30	−0.30 ± 0.50**

Note: Significant difference between the fixed and free-floating stretcher mechanisms: *$P < 0.05$, **$P < 0.01$.
Abbreviations: P^{ap}_{handle} and P^{vert}_{handle}: power delivered at the handle in the antero-posterior and vertical directions; $P^{ap}_{stretcher}$: power delivered at the stretcher in the antero-posterior direction; and P_{ext}: external power.

supplied by P^{ap}_{handle}. $P^{ap}_{stretcher}$ and P^{ap}_{handle} maximum values represented 38.5% and 75.0% of the P_{ext} maximum value, respectively.

Compared with the fixed condition, the P_{ext} maximum value occurred at the same stage of the cycle ($P > 0.05$) but was 12.6% lower ($P < 0.01$). Conversely, the whole of the recovery phase showed larger negative values [lower minimum value of 40% ($P < 0.01$)]. This absorbing power arose from both P_{handle} and $P_{stretcher}$ data. The average power was 8.5% lower ($P < 0.01$) when the rower used the free-floating mechanism (554 ± 63 W) than the fixed mechanism (507 ± 74 W).

Unnecessary movement at the catch

At the catch, the force produced by the rower is used to accelerate the rower's centre of mass and the stretcher mechanism in opposite directions or is transferred to the ergometer flywheel via the handle or stretcher mechanism. However, this force cannot be transferred immediately to the ergometer flywheel. A force on the handle can only be generated when the difference in velocity between the handle and the stretcher (which is zero by definition at the catch) is superior to the translational equivalent of the flywheel velocity. As a result, an unecessary movement following the catch was observed when no handle force was produced for both ergometer conditions.

As the stretcher is stationary on the fixed ergometer, the force produced by the rower on the stretcher during this unnecessary movement is used to accelerate the rower's centre of mass backwards. The lower limb extension is coupled to the rower's centre of mass motion and so the acceleration generated depends on body mass.

On the free-floating ergometer, the velocity of the handle relative to the stretcher was found to be greater during the first 0.16 m of the propulsion length. When no handle force is collected, one part of the force generated on the stretcher is used to accelerate the rower's centre of mass backwards; the other part is used to accelerate the stretcher mechanism's centre of mass forwards. The lower limb extension can be then associated with a minimal acceleration of the rower's centre of mass.

The faster increase in velocity difference between handle and stretcher for the floating condition is a consequence of the greater antero-posterior acceleration of the stretcher mechanism during the free-floating condition than the rower's centre of mass antero-posterior acceleration in the fixed condition, as the mass of the stretcher mechanism was approximately 4.5 times less than the mass of the power. Figure 9 provides support for this hypothesis and shows that $a^{ap}_{stretcher}$ in the floating condition was

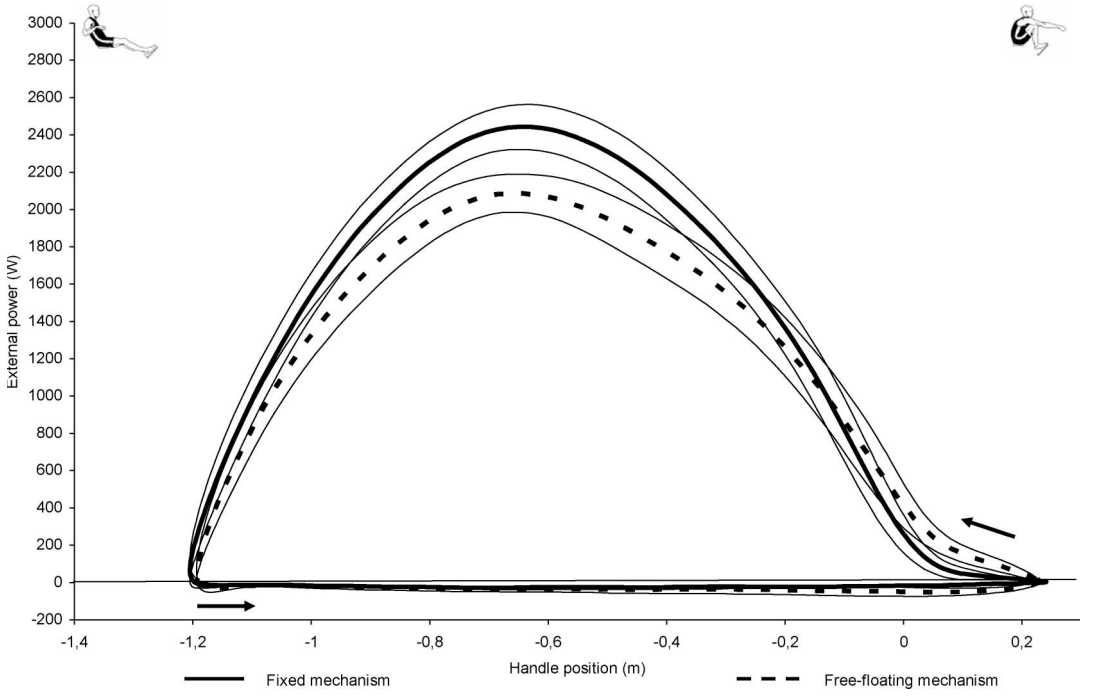

Figure 8. Mean curves of the external power generated by the 25 rowers (P_{ext}) as a function of handle position. Figures of the rower indicate the catch and finish positions; the arrows indicate the way of reading the curves from these two positions.

significantly different than a^{ap}_{COM} in the fixed condition for the first 0.34 m of the propulsion phase; $a^{ap}_{stretcher}$ was significantly greater than a^{ap}_{COM} after a handle displacement of 0.06 m from the catch.

Discussion

Significant mechanical differences among the two stretcher conditions were observed. The patterns of force–handle position and power–handle position curves are clearly specific to each mechanism rowed. The maximum forces, the maximum external powers and the average external powers are significantly more important when the fixed stretcher mechanism is used. These differences are caused by the inertial force created by the rower during the transition between the phases of the rowing motion. The displacements of the rower's centre of mass are much more important on the fixed stretcher mechanism. The catch and the finish of the cycle are characterized by consistently larger contact forces with the fixed stretcher. The rower must therefore produce larger antero-posterior force at the stretcher to accelerate his centre of mass in the positive and negative directions throughout the cycle to maintain a specific cycle rate. As shown by the free body diagram, it also requires a larger vertical stretcher force to balance the clockwise moment generated.

The results of this study suggest that a lower inertial force is necessary to accelerate the segments of the rower, thus causing a faster transfer to the force generated at the handle for the free-floating ergometer. The fastest increase in F^{ap}_{handle} with the free ergometer is due to the involvement of the lower limbs at the beginning of the propulsion phase. Furthermore, the back and the upper limbs are involved more in the fixed condition at the end of the propulsion phase. Rowing with a free mechanism seems to require different muscular coordination to produce external force contact patterns. Consequently, for a set-up dedicated to intense ergometer training, the use of one of the mechanisms rather than the other could have a different impact on the physiological muscle adaptations, as shown by Roth, Schwanitz, Pas and Bauer (1993), and on the pattern of muscle group recruitment (Green & Wilson, 2000).

The lower catch and maximum values for external contact forces with the free-floating stretcher mechanism could decrease the risk factors for injuries. An inverse dynamic analysis may show that the rower generates lower catch and maximum values for the joint mechanical actions (net joint forces and net joint moments) during the free-floating condition. The net moments produced at each joint of the rower are required to cause the linear acceleration of the rower's centre of mass and angular acceleration of each segment. Their results are also the external contact forces.

At the catch, no handle force was generated by the rower. As a result, the mechanical actions at the sacroiliac joint, the most common site of injury in

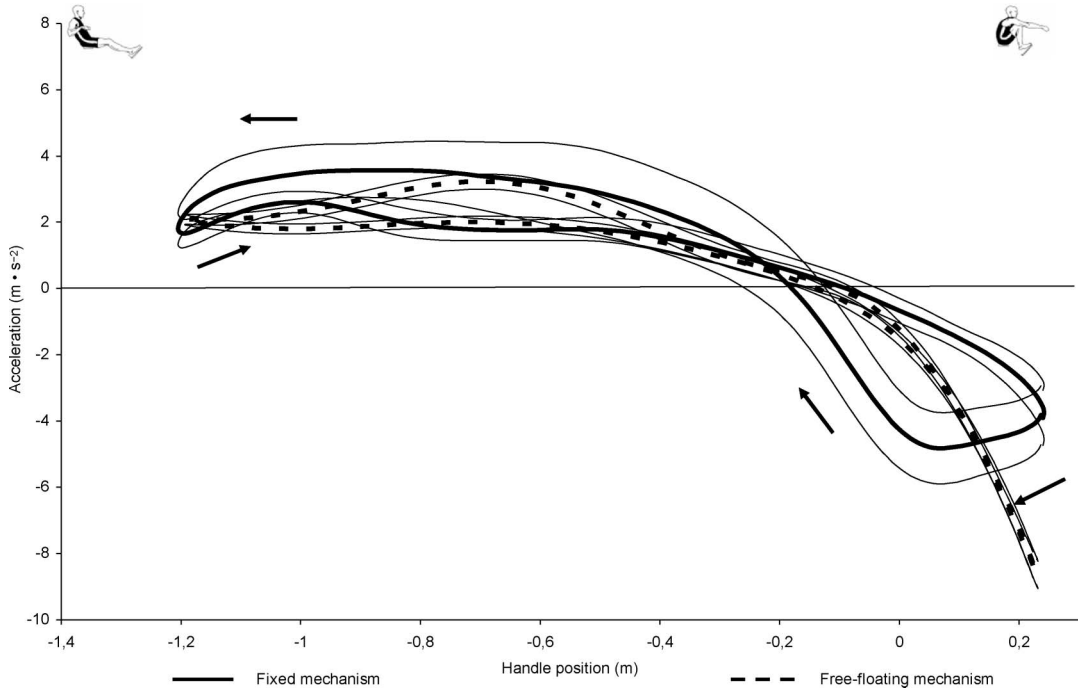

Figure 9. Mean curves of the rower's centre of mass antero-posterior acceleration (a^{ap}_{COM}) during the fixed condition and stretcher mechanism antero-posterior acceleration ($a^{ap}_{stretcher}$) during the free-floating condition produced by the 25 rowers as a function of handle position. The $a^{ap}_{stretcher}$ curve was reversed for easy comparison with the a^{ap}_{COM} curve. Figures of the rower indicate the catch and finish positions; the arrows indicate the way of reading the curves from these two positions.

rowing (Shephard, 1998), should be largely determined by the inertial forces generated by the trunk, head and upper limbs. The larger acceleration of the rower's centre of mass required at the catch for the fixed ergometer should result in larger mechanical actions. The acceleration of the rower's centre of mass overestimates the acceleration of the trunk, head and upper limbs. However, it highlights the main differences between the two conditions for the inertial contribution to the net sacroiliac moment. Furthermore, the mechanical actions produced at the lower limb joints should be mainly related to the stretcher force. The acceleration of the rower's centre of mass does not reflect the linear acceleration of the lower limb segments. The flexion/extension movements of the lower limbs are only coupled to the acceleration of the rower's centre of mass for the fixed condition. When the free-floating stretcher mechanism is rowed, the centre of mass of the lower limb segments and the rower's centre of mass are accelerated in opposite directions throughout the rowing cycle. These statements suggest that the passive structures of the rower's joints (ligaments, tendons, capsules) could be loaded less at the catch of the cycle on the floating stretcher, when the lower limb joints and trunk are fully flexed. This is especially important at the level of the sacroiliac joint, as low activation of the back extensor muscles has been reported at the catch (Caldwell, McNair, & Williams, 2003).

Moreover, we can expect that the rower generates lower maximum mechanical actions with the free-floating mechanism. Recently, Colloud, Champely, Bahuaud and Chèze (2002) examined the flexion/extension ranges of motion of the whole body when rowing the two stretcher mechanisms. They found closed curve patterns during the whole rowing cycle for these two conditions. The duration of the propulsion phase in our study was similar for both conditions, thus the joint angular velocities should be equivalent throughout the rowing cycle. As the rower's centre of mass acceleration is low when stretcher and handle maximum forces occurred, peak mechanical actions should be mainly related to the magnitude of the external contact forces. The lower average power associated with the free-floating condition supports the lower generation of mechanical actions.

Conclusions

This study has shown that elite rowers using a free-floating stretcher mechanism produce different shapes of force–handle position and power–handle position curves than when using the fixed mechanism. These differences were mainly caused by the

inertial forces created during the transition between phases. Our results suggest that the change in inertia forces between the two conditions may have implications for the recruitment timing and/or order of the major muscular groups involved in ergometer rowing, as well as for catch and maximum values of the mechanical actions generated at each joint of the rower. However, further study must be undertaken to support the validity of these hypotheses, such as inverse dynamic and/or electromyograpic analysis.

Acknowledgements

We wish to thank Charles Imbert and Luc Montigon (Pôle France Aviron Lyon), Élie Darré and Alain Waché (Aviron Grenoblois) for providing invaluable help with this study as well as the anonymous reviewers for their constructive comments and suggestions regarding the manuscript. We greatly appreciated the cooperation and the enthusiasm of those who participated in this study.

References

Caldwell, J. S., McNair, P. J., & Williams, M. (2003). The effect of repetitive motion on lumbar flexion and erector spinae muscle activity in rowers. *Clinical Biomechanics*, *18*, 704–711.

Colloud, F., Champely, S., Bahuaud, P., & Chèze, L. (2002). Kinematic symmetry in rowing: Comparison of fixed versus free-floating ergometer. In K. E. Gianikellis (Ed.), *Scientific Proceedings of the XXth International Symposium on Biomechanics in Sports* (pp. 275–278). Universitad de Extremadura, Spain.

Green, R. A. R., & Wilson, D. J. (2000). A pilot study using magnetic resonance imaging to determine the pattern of muscle group recruitment by rowers with different levels of experience. *Skeletal Radiology*, *29*, 196–203.

Hartman, U., Mader, A., Wasser, K., & Klauer, I. (1993). Peak force, velocity, and power during five and ten maximal rowing ergometer strokes by world class female and male rowers. *International Journal of Sports Medicine*, *14*(suppl. 1), 42–45.

Hawkins, D. (2000). A new instrumentation system for training rowers. *Journal of Biomechanics*, *33*, 241–245.

Lamb, D. H. (1989). A kinematic comparison of ergometer and on-water rowing. *American Journal of Sports Medicine*, *17*, 243–247.

Macfarlane, D. J., Edmond, I. M., & Walmsey, A. (1997). Instrumentation of an ergometer to monitor the reliability of rowing performance. *Journal of Sports Sciences*, *15*, 167–173.

Mahony, N., Donne, B., & O'Brien, M. (1999). A comparison of physiological responses to rowing on friction-loaded and air-braked ergometers. *Journal of Sports Sciences*, *17*, 143–149.

Martindale, W. O., & Robertson, D. G. E. (1984). Mechanical energy in sculling and in rowing an ergometer. *Canadian Journal of Applied Sports Sciences*, *9*, 153–163.

Millward, A. (1987). A study of the forces exerted by an oarsman and the effect on boat speed. *Journal of Sports Sciences*, *5*, 93–103.

Nolte, V. (1991). Introduction to the biomechanics of rowing. *FISA (Fédération Internationale des Sociétés d'Aviron) Coach*, *2*(1), 1–6.

Pudlo, P., Barbier, F., & Angue, J. C. (1996). Instrumentation of the Concept II ergometer for optimization of the gesture of the rower. In S. Haake (Ed.), *The Engineering of Sport: Proceedings of the International Conference on the Engineering of Sport* (pp. 137–140). Balkerma: Rotterdam, The Netherlands.

Richards J. G. (1999). The measurement of human motion: A comparison of commercially available systems. *Human Movement Science*, *18*, 589–602.

Roth, W., Schwanitz, P., Pas, P., & Bauer, P. (1993). Force–time characteristics of the rowing stroke and corresponding physiological muscle adaptations. *International Journal of Sports Medicine*, *14*(suppl. 1), 32–34.

Secher, N. H. (1993). Physiological and biomechanical aspects of rowing: Implications for training. *Sports Medicine*, *15*, 24–42.

Shephard, R. J. (1998). Science and medicine of rowing. *Journal of Sports Sciences*, *16*, 603–620.

Steinacker, J. M. (1993). Physiological aspects of training in rowing. *International Journal of Sports Medicine*, *14*(suppl. 1), 3–10.

Steinacker, J. M., Lormes, W., Lehmann, M., & Altenburg, D. (1998). Training of rowers before world championships. *Medicine and Sciences in Sports and Exercises*, *30*, 1158–1163.

Torres-Moreno, R., Tanaka, C., & Penney, K. L. (2000). Joint execution, handle velocity, and applied force: A biomechanical analysis of ergonometric rowing. *International Journal of Sports Medicine*, *21*, 41–44.